

Article

# The Change of Microstructure and Hardness of Duo-Casted Al3003/Al4004 Clad Material during Extrusion Process

Jin-Kyung Lee <sup>1</sup>, Sang-Pill Lee <sup>1</sup>, Jong-Sup Lee <sup>2</sup>, Sangmok Lee <sup>2,\*</sup>, Ilguk Jo <sup>3,\*</sup> and Dong-Su Bae <sup>3,\*</sup>

<sup>1</sup> Division of Mechanical, Automobile, Robot Component Engineering, Dong-Eui University, Busan 47340, Korea; leejink@deu.ac.kr (J.-K.L.); splee87@deu.ac.kr (S.-P.L.)

<sup>2</sup> Advanced Forming Technology Center, Korea Institute of Industrial Technology, Inchoen 21999, Korea; jongsup@kitech.re.kr

<sup>3</sup> Division of Advanced Materials Engineering, Dong-Eui University, Busan 47340, Korea

\* Correspondence: sangmokl@kitech.re.kr (S.L.); ijo@deu.ac.kr (I.J.); dsbae@deu.ac.kr (D.-S.B.); Tel.: +82-51-890-2288 (D.-S.B.)

Received: 27 October 2020; Accepted: 6 December 2020; Published: 7 December 2020



**Abstract:** This study was carried out to observe and measure the microstructure, distance between dendrite arms, aspect ratio, and Knoop hardness change of extruded material formed by the hydro co-extrusion of Al3003/Al4004 clad material manufactured by the duo-casting method. The specimen of duo-casted Al3003/Al4004 clad materials was circle shaped; it was composed of Al3003 (outside) and Al4004 (inside) materials. The manufacturing conditions of the hydro co-extruded specimen were 423 K temperature and 6.5 ratio of extrusion. At the interface of the duo-casted Al3003/Al4004 clad material, a non-junction at the interface and non-metallic inclusions of Si- and Mn-based oxides were observed. Al3003 exhibits equiaxed crystals; Al4004 has a casted structure with dendrites before extrusion, showed slight deformation during extrusion, and then finally exhibited completely deformed structures after extrusion. In the cast material, the distance between dendrite arms increased, and the aspect ratio of dendrites tended to decrease from the surface to the center. However, in the case of the extruded material, neither Al3003 nor Al4004 changed significantly from the surface to the inside. As extrusion progressed, the Knoop hardness value at the interface of Al3003/Al4004 increased rapidly compared with those of Al3003 and Al4004 matrixes.

**Keywords:** duo-casted Al3003/Al4004 clad materials; extrusion process; microstructure property; knoop hardness

## 1. Introduction

Clad materials are a variant of typical composites that consist of two or more materials joined at interface surfaces. As metallic composite materials, clad materials are developed for the needs of users because single metals often cannot satisfy the application conditions. Recently, several methods such as rolling, explosive welding, extrusion, drawing, hot pressing, and duo-casting have been used for clad material production [1–12].

Al3003 alloy is an Al-Mn alloy and contains mainly Mn 1.3%. It has excellent corrosion resistance, good stress corrosion cracking property, formability, solderability, weldability and forgeability, and it has low mechanical strength and high ductility [13,14]. On the other hand, Al 4004 alloy is an Al-Si-based alloy; when its Si content is increased by 12% or more, then its melting point decreases. However, when Si is added within a certain range, the fluidity of the molten state is improved, and cracks hardly occur during solidification when Si is added within a range. Only the property of

stress corrosion cracking is good, but the corrosion resistance, solderability, and weldability are bad; furthermore, the material has mechanical properties of high strength and hardness and low ductility compared to those of Al3003 alloy [15–18].

When clad materials are manufactured by rolling, drawing, and hot pressing processes, oxides are easily formed on the metal surfaces and remain on the joining interface. This has a negative effect of reducing the bond strength [7,8,12]. Therefore, in the case of clad cast materials formed by the duo-casting process, unlike the warm rolling process, the bonding interface is manufactured in a bonded state, and thus there is an advantage of avoiding oxidation reaction with the atmosphere [9–11].

Some research papers have been published on microstructural characteristics of round bars of Al3003/Al4004 clad materials manufactured using various casting methods [9,19,20]. To use such a clad material as an industrial structural material, extrusion needs to be conducted; however, research on the extrusion of Al3003/Al4004 clad material is very limited. Son et al. revealed that the hardness of the extrusion of Al3003/Al4004 clad material increased in the shape of the parabola toward the center before the extrusion; however, after the extrusion, Al4004 showed almost a constant hardness. However, no research results on the microstructure and hardness changes of Al3003/Al4004 clad during the actual extrusion process have been published yet.

In this study, Al3003/Al4004 clad material was manufactured by placing a forming Al3003 alloy, with high corrosion resistance, on the outside and Al4004 alloy, with low corrosion resistance and high strength, on the inside by the duo-casting method [9]. The microstructure and micro-hardness properties of hydro co-extruded Al3003/Al4004 material with duo-casted Al3003/Al4004 clad material were analyzed. The purpose of this study was to secure the basic data of the microstructure and hardness change of duo-casted Al3003/Al4004 clad material formed by extrusion processing.

## 2. Materials and Methods

Al3003 alloy as the outer layer and Al4004 alloy as the inner layer were used for the electromagnetic duo-casting process. The experimental apparatus for the duo-casting consisted of ultrasonic and electromagnetic stirring equipment, a temperature measurement system, and two resistance furnaces. First, Al3003 alloy melt was poured into the mold and formed a solidified shell; then, Al4004 melt was poured into the solidified shell of Al3003, followed by electromagnetic stirring during solidification [9]. Figure 1 shows the dimensions and sampling positions of the duo-casted clad material. Figure 1a shows a cross-section of the cast material of the duo-casted Al3003/Al4004; this sample was made in a circle shape at Dailen University of Technology (China) by the electromagnetic duo-casting method. Figure 1b shows the location of the sample collection used in this study. The manufactured clad ingot was 150 mm in diameter and 315 mm in length; it was cut from the cross-section of the ingot. The specimen was cut and collected at the location shown in Figure 1b, using as a clad material a 10 mm thick disk. That is, sampling number 1 was taken from the surface portions of Al3003, specimens 2 and 3 were taken from the boundary of Al3003 and Al4004, and specimens 4 and 5 were taken from the middle and central portions of Al4004.

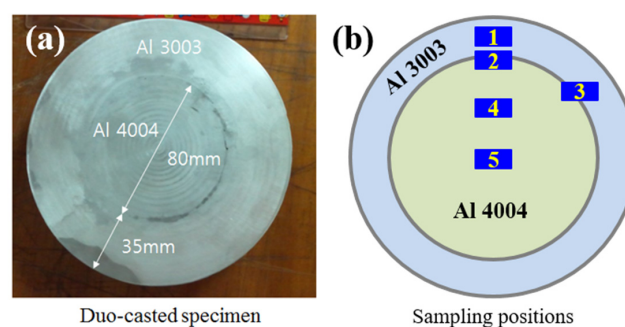


**Figure 1.** (a) Dimension and shape, and (b) specimen sampling positions of an electromagnetic duo-casted Al3003/Al4004 clad material.

A hydrostatic pressure extrusion test is carried out by attaching the HCE (Hydro co-extrusion equipment) chamber, with maximum plasticity of 1000 MPa, to a 5000 tonne hydraulic press. A picture of the press with HCE equipment and a conceptual sketch of the HCE chamber are shown in Figure 2. To manufacture extrusion specimens for HCE, a 150 mm diameter clad ingot was machined into a specimen for hydrostatic pressure extrusion with a diameter of 100 mm and a length of 100 mm (Figure 2c). The extrusion specimen, which is tangential to the die, was cut to an angle of 45°; to avoid adhesion between the mold and the extrusion material, the buffer pad was manufactured with Al1050 with a thickness of 10 mm. The clad specimen was inserted into the buffer pad, which was followed by the HCE test. The casting speed was 55 mm/min and the pouring temperatures of the Al3003 and Al4004 material were 993 K and 903 K, respectively. The casting temperature was determined by considering the solidus and liquidus temperatures of Al3003 and Al4004.

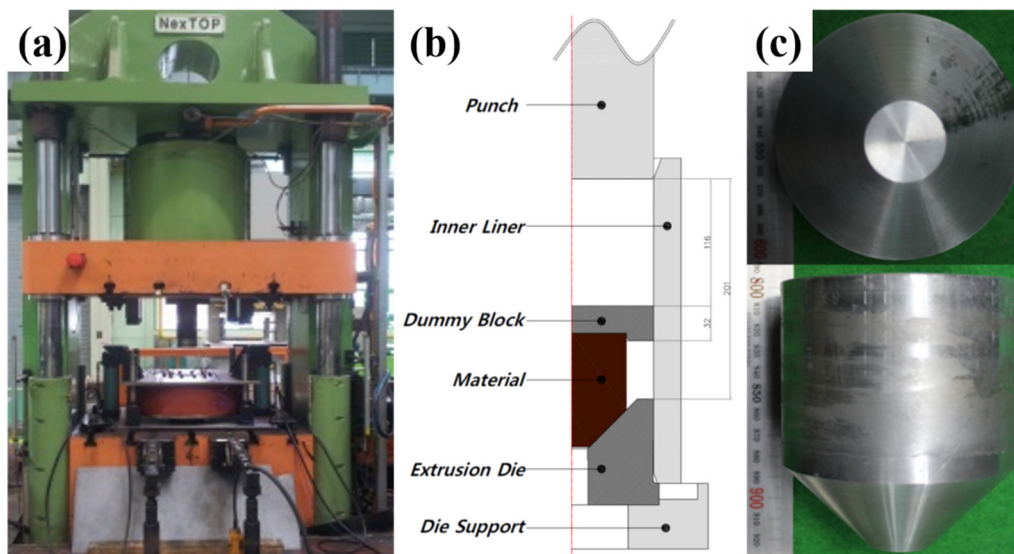


**Figure 2.** (a) Hydro co-extrusion equipment (HCE), (b) schematic diagram of HCE chamber, and (c) shape of prepared specimen and its dimensions for HCE process.

Table 1 shows details of the manufacturing conditions of the hydro co-extruded specimen which were 423 K in temperature and 6.25 in the ratio of extrusion, respectively.

**Table 1.** Hydro co-extrusion process parameters.

Conditions	Extrusion Temp. [K]	Initial Billet Diameter [mm]	Extrusion Die Diameter [mm]	Extrusion Ratio	Half Die Angle [deg.]
Values	423	100	40	6.25	45

The Knoop hardness (HK) tester was used to measure the micro-hardness change of the Al3003/Al4004 clad specimen with the extrusion process. To obtain reliable data, a total of 12 indentations were made on each specimen, and hardness values were statistically averaged.

Microstructures of each Al3003/Al4004 clad were observed using an Optical Microscope (OM); the grain size, dendrite arm distance, and aspect ratio of the dendrite structure were measured by image analysis. For each of the specimens, dendrite arm distance values were measured using an image program by taking 9 measurements, and statistical evaluation was performed. In general, aspect ratio is used to specify the shape of particles. In this study, aspect ratio was used to indicate the shape of the dendrite structure. The closer the aspect ratio is to 1, the more the dendrite phases have an equiaxed microstructure; the smaller the aspect ratio is, and the more the dendritic structures have a needle-like

shape. Scanning Electron Microscope (SEM, Quanta 200 FEG) and Energy Dispersed X-ray point (EDX, Genesis XM2, resolution 129 eV or less) analyses were conducted on non-metallic inclusions at the interfaces of the specimens to examine the bonding interface properties of the Al3003/Al4004 clad material. The specimens from the co-extruded materials for the mechanical property test and microstructure analysis were cross-sectioned parallel to the extrusion direction and prepared using standard metallographic procedures.

### 3. Results and Discussion

#### 3.1. Microstructure of Cross Section

Figure 3 shows the results of OM observation of the as-casted microstructure in specimen numbers 1 to 5 along the cross-section. A typical cast morphology with large numbers of dendrites in the entire specimen was found. A eutectic structure, which resulted from the cooling of remaining liquid phases, was also observed.

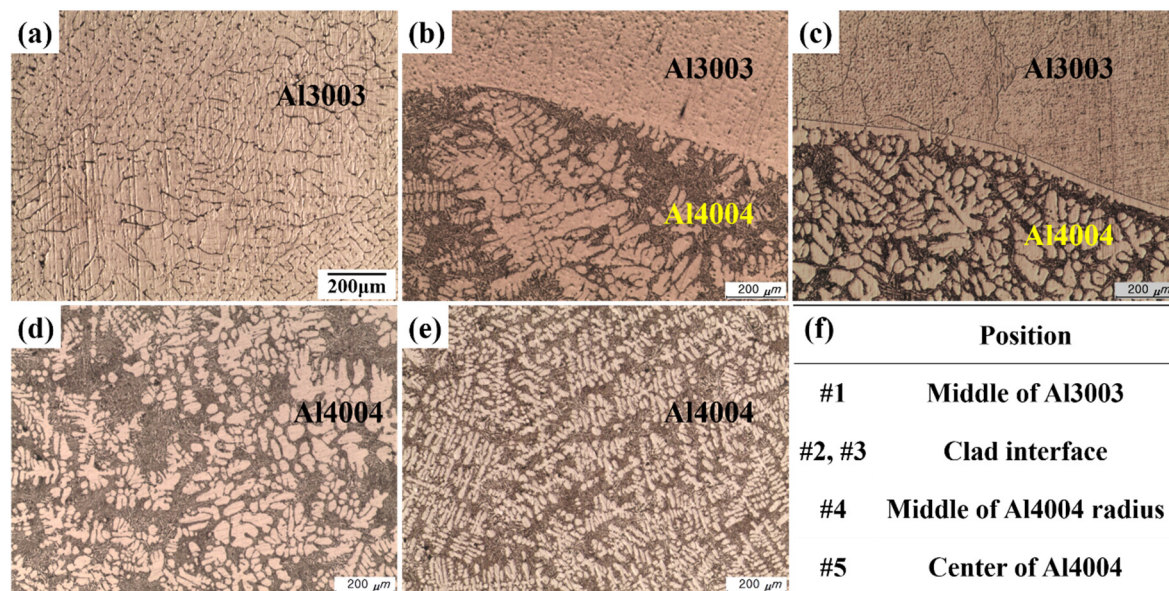
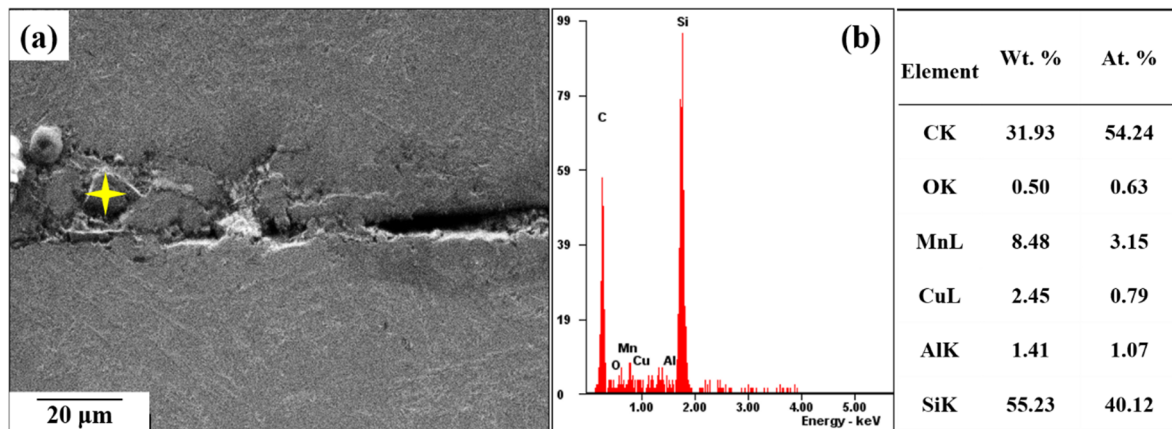


**Figure 3.** As-received microstructures of duo-casted Al3003/Al4004. Sampling positions (a) #1 in Al3003, (b) #2 in Al3003/Al4004, (c) #3 in Al3003/Al4004, (d) #4 in Al400, and (e) #5 in the Al4004 region, and (f) sampling positions (same magnification).

Figure 3a shows the surface microstructure of the Al3003 material, which is the outer region of the duo-casted Al3003/Al4004 clad material. Figure 3b,c show the interface area of the Al3003/Al4004 clad material. In Figure 3d,e, an Al + Si eutectic structure is formed between the typical dendrites of proeutectic  $\alpha$ ; the size of the dendrites and the eutectic structure turn out that it becomes fine compared with those shown in Figure 3a–c. In the microstructural analysis, a typical cast morphology with eutectic structure and dendrite with proeutectic  $\alpha$  phase were observed in all parts except the surface of the duo-cast material [9,10]. At the surface part of the casted material, a proeutectic  $\alpha$  phase with a grain size of about 63  $\mu\text{m}$  was observed; the other part was found to be an  $\alpha$  phase with a eutectic structure and dendrites. As can be seen in Figure 3d,e, the center of Al4004 had more fine and needle-like dendritic structures. This is attributed to forced convection from electromagnetic stirring (EMS), which caused a structural transformation from dendrites to irregular fine grains (Figure 3d). However, the dendritic structure at the center is maintained (Figure 3e), which indicates that EMS does not affect the center of the specimen.

As can be seen in Figure 4, there are some impurities and non-bonded portions at the interface of Al3003/Al4004, although OM showed a good bonding interface. These impurities, observed by EDS

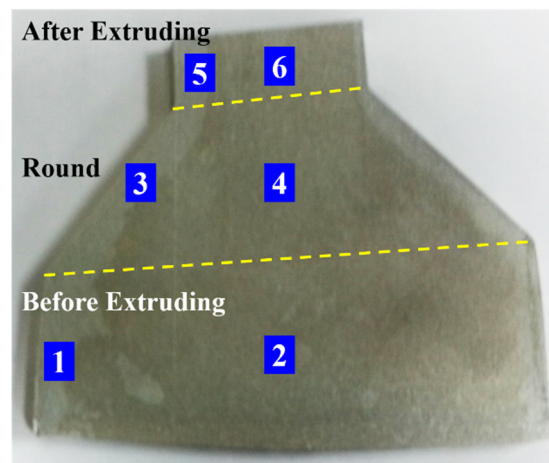
point analysis, were non-metallic inclusions of Si- and Mn-based oxides, which are expected to reduce the bond strength at the interface of the clad material [7,8].



**Figure 4.** (a) SEM images of non-metallic inclusion at interface of Al3003 and Al4004 boundary in sampling position #3 of as-received duo-casted Al3003/Al4004, and (b) Energy Dispersed X-ray point (EDS) pattern and composition of the inclusion.

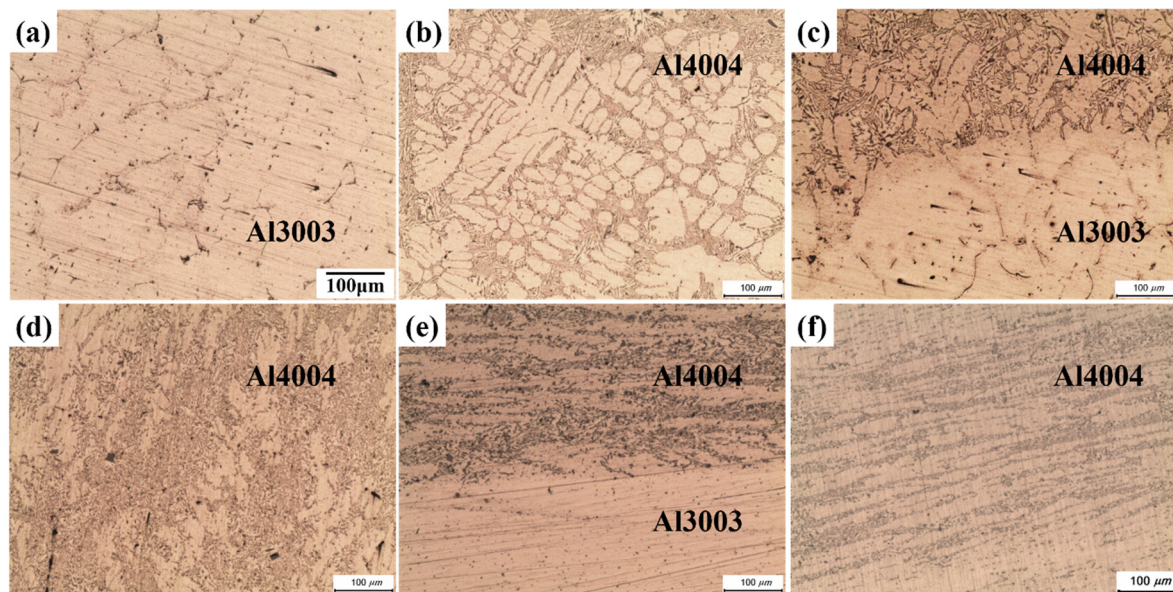
### 3.2. Structure Change and Hardness Change before and after Extrusion

Figure 5 shows the duo-casted Al3003/Al4004 clad material during the extrusion process. Extrusion was stopped to obtain specimens to be extruded before (1, 2), during (3, 4), and after extrusion (5, 6). Specimen 1 was taken from Al3003 before extrusion; specimens 3 and 5 were taken at the interface of Al3003/Al4004 during and after extrusion, respectively. Specimens 2, 4, and 6 were taken from the center of Al4004 before, during, and after extrusion. Changes of microstructure and Knoop hardness before, during, and after extrusion were observed and measured using these specimens.



**Figure 5.** Shape of hydro co-extruded duo-casted Al3003/Al4004 and sampling positions with numbers (1,2: Before extruding/3,4: round/5,6: after extruding).

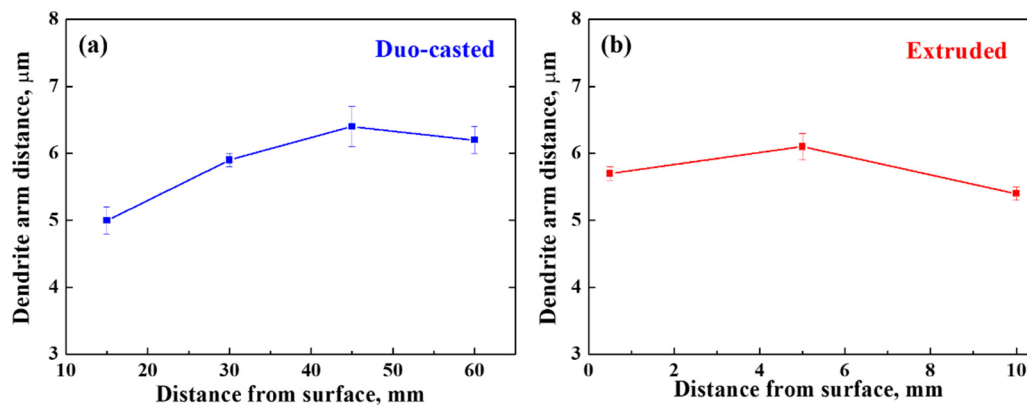
Figure 6a shows OM photographs of the Al3003 area before the extrusion of specimen No. 1; (b) shows the Al4004 before the extrusion of specimen No. 2; (c) shows Al3003/Al4004 interface during the extrusion of specimen No. 3; (d) shows Al4004 during the extrusion of specimen No. 4; (e) shows the Al3003/Al4004 interface after the extrusion of No. 5 specimen; and (f) shows Al4004 after the extrusion of No. 6 specimen.



**Figure 6.** Microstructures of duo-casted Al3003/Al4004. Sampling positions (a) #1 in Al3003, (b) #2 in Al4004 before the extruding region, (c) #3 in Al3003/Al4004, (d) #4 in Al4004 of the round region, (e) #5 in Al3003/Al4004, and (f) #6 in Al4004 after extrusion (same magnification).

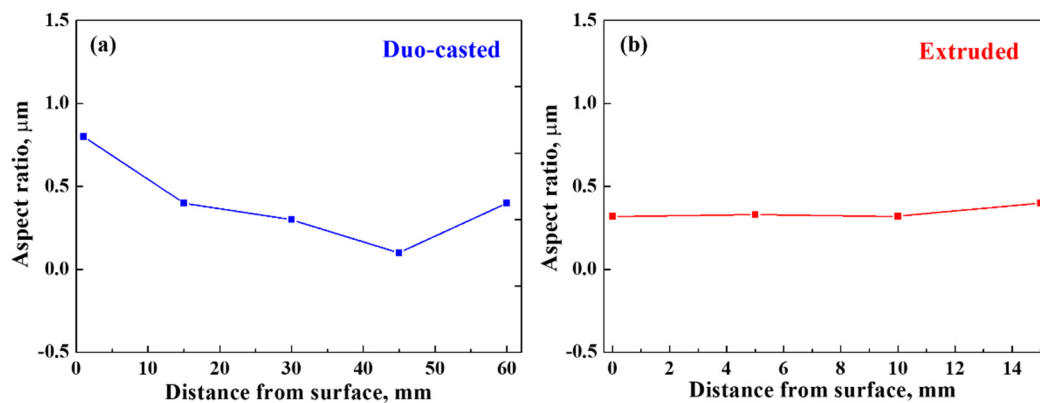
In the structure before extrusion (Figure 6a,b), Al3003 shows equiaxed crystals, and Al4004 shows dendrites. During extrusion (Figure 6c,d), the equiaxed crystals of Al3003 and the dendrites of Al4004 are slightly deformed. However, after extrusion (Figure 6e,f), the equiaxed crystals of Al3003 and the dendrites of Al4004 exhibited long stretches in the extrusion direction due to the extrusion, so that their original shapes could not be determined. Especially, good adhesion between Al4004 and Al3003 materials was obtained at the interfacial region of the extruded Al3003/Al4004 clad materials due to the significant plastic deformation of the base metals.

Figure 7a shows image analysis results of the distance between dendrite arms of duo-casted material; Figure 7b shows extruded Al3003/Al4004 clad material. As shown in Figure 7a, the distance between dendrite arms of duo-casted Al3003/Al4004 clad material tended to increase gradually from the surface to the center. On the other hand, the distance between the dendrite arms from the surface to the center of the extruded material, as shown in Figure 7b, did not significantly change. In other words, it can be seen that the distance between dendrite arms is distributed at uniform intervals throughout the entire extrusion material by extrusion processing.



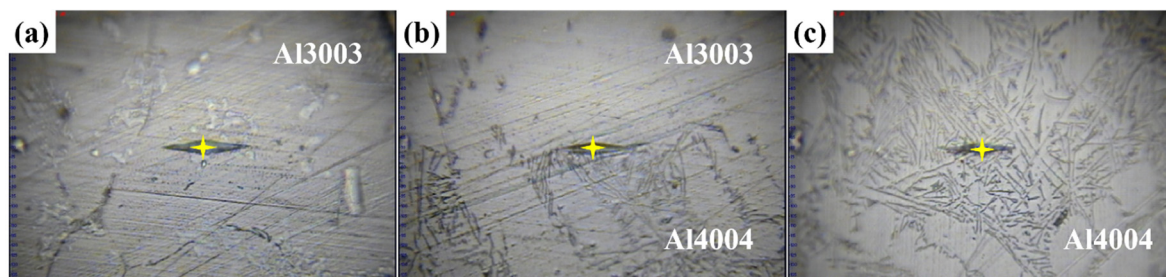
**Figure 7.** Distribution of dendrite arm distance for (a) duo-casted and (b) extruded Al3003/Al4004 clad material.

Figure 8 shows image analysis results of the aspect ratio of dendrites in (a) duo-casted and (b) extruded Al3003/Al4004 clad material. As can be seen in Figure 8a, the aspect ratio of dendrites in the duo-casted material gradually decreases from the surface to the center. This means that the shape of the dendrites changes from equiaxed to long axis (needle-like) shape. It can be seen that in the area closest to the surface of the casting mold, the secondary dendrite arm was destroyed by the influence of EMS, which resulted in the equiaxed microstructure; the effect of EMS on the shape of the dendrite phase gradually decreases to the middle of the ingot. Figure 3e shows the center part of the ingot, which is not affected by EMS and has a secondary dendrite arm remaining without deformation. Therefore, the aspect ratio of the dendritic structure measured in the center part is considered to be slightly higher than that measured in the middle, where the secondary dendrite arm was destroyed. As shown in Figure 8b, in the case of the extruded material, the aspect ratio did not change significantly from the surface to the center, unlike the cast material. That is, dendrites with a long axis became of uniform shape and were distributed over the entire extruded material by the extrusion process. In Figures 7 and 8, it can be seen that the aspect ratio and the dendritic arm distance of the clad material with an extrusion ratio of 6.25 showed a constant value, but the values decreased overall compared to those of the cast materials.



**Figure 8.** Distribution of aspect ratio of dendrites for (a) duo-casted and (b) extruded Al3003/Al4004 clad material.

Figure 9 shows example of measurements of Knoop microhardness in the Al3003 matrix, Al3003/Al4004 junction interface, and Al4004 matrix in the round section during extrusion. Under the same hardness measurement conditions, the indentation size of the Knoop indenter at the Al4004 matrix is very small compared to those of Al3003 and the Al3003/Al4004 interface. These results are shown in Figure 10 as the Knoop hardness change at each site before, during, and after extrusion. As shown in Figure 10, the hardness increases due to work hardening as the extrusion proceeds.



**Figure 9.** Examples of Knoop indenter traces on (a) Al3003 matrix, (b) Al3003/Al4004 interface, and (c) Al4004 matrix of round region during extrusion.

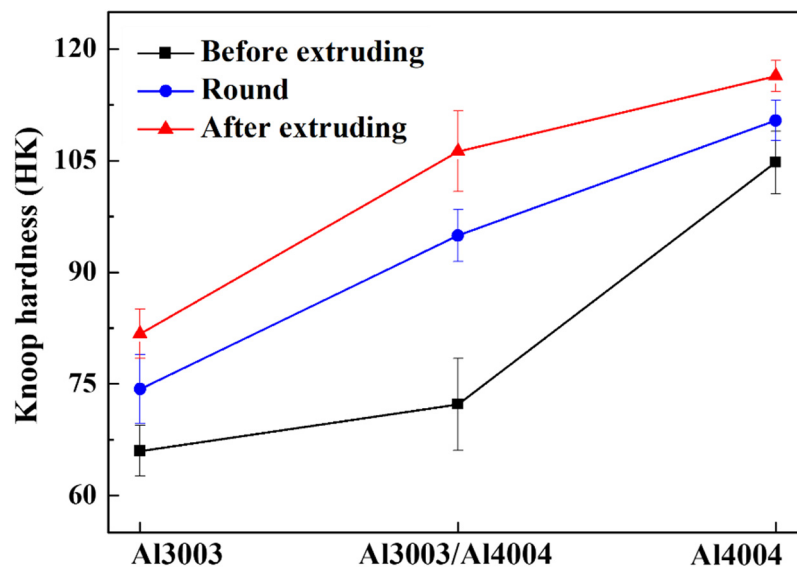


**Figure 10.** Changes of Knoop hardness in Al3003, Al3003/Al4004, and Al4004 parts before, during (round), and after extrusion.

Differences in hardness values before and after extrusion were 15.7 for Al3003, 34.0 for Al3003/Al4004, and 11.6 for Al4004. That is, increases of hardness by work hardening are not so different. On the contrary, it can be seen that the hardness value at the boundary of Al3003/Al4004 increases approximately 2.2 and 2.9 times compared to the hardness values of Al3003 and Al4004, respectively. This is because most of the plastic deformation occurred at the boundary of Al3003/Al4004 by the extrusion process [9], where the ductile Al3003 material of the surface portion acted as lubricating oil; the plastic deformation of the extrusion process occurred mainly at the interfacing region of the Al3003 and Al4004 materials. It can be seen that the hardness increases rapidly due to the increase in the contribution to work hardening according to the increase in the amount of plastic deformation. In all the processes before, during, and after extrusion, the hardness value of Al3003 is the lowest, and the hardness value of Al4004 is the highest. With the extrusion process, the interfacial hardness of the Al3003/Al4004 clad increased; this is attributed to the elimination of macropores at the interface during extrusion [10]. However, if an impurity such as oxide exists in the interface, as shown in Figure 4, under some extrusion conditions, cracks could form due to oxide breakage from the extrusion deformation, which might lead to the formation and propagation of micropores due to differences in plastic deformation characteristics. This could degrade the ductility of the extruded material.

#### 4. Conclusions

In this study, the microstructure and Knoop hardness of the hydro co-extruded Al3003/Al4004 clad material, manufactured by the electromagnetic duo-casting method, was investigated. Obtained results are outlined below.

- At the surface of the casting material, a proeutectic  $\alpha$  phase with a grain size of about 63  $\mu\text{m}$  was observed; in all other parts, a proeutectic  $\alpha$  phase and dendrites were observed.
- Al3003 exhibits equiaxed crystals and Al4004 has a casted structure with dendrites before extrusion; this shows that there was slight deformation during extrusion. Then, finally, the material exhibited completely deformed structures after extrusion.
- The distance between the dendrite arms of the casting material increased from the surface to the inside; however, in the case of the extruded material, the distance between dendrite arms did not change from the surface to the center. The aspect ratio of dendrites for the cast material tended to decrease from the surface to the center; however, throughout the extruded material, the aspect ratio did not change significantly.

- As extrusion progressed, the Knoop hardness values of Al3003, the Al3003/Al4004 interface, and Al4004 increased due to work hardening. Hardness values at the boundary of Al3003/Al4004 increased approximately 2.2 and 2.9 times compared with those of the Al3003 and Al4004 matrixes, respectively. The hardness value of Al 3003 was the lowest, and that of Al4004 was the highest.
- After the extrusion process, the Knoop hardness of the Al3003/Al4004 clad interface increased; the existence of oxides at the interface could deteriorate the mechanical properties of the extruded parts.
- The aspect ratio and the dendrite arm distance from extrusion show constant values; it can be seen that overall, reduction has been achieved in the clad material compared to the cast material. The hardness has increased due to work hardening.

**Author Contributions:** Conceptualization, D.-S.B.; Data curation, S.-P.L.; Formal analysis, J.-K.L.; Funding acquisition, I.J.; Investigation, S.-P.L. and J.-S.L.; Methodology, S.L.; Project administration, I.J.; Supervision, D.-S.B.; Validation, S.L.; Visualization, J.-S.L.; Writing—original draft, J.-K.L.; Writing—review and editing, D.-S.B. All authors have read and agreed to the published version of the manuscript.

**Funding:** This research was supported by National R&D Program through the National Research Foundation of Korea(NRF) funded by Ministry of Science and ICT (NRF-2020M3H4A3105945). This research was also supported by the Basic Science Research Capacity Enhancement Project through a Korea Basic Science Institute (Core-facility for Converging Materials) grant funded by the Ministry of Education (2019R1A6C1010045).

**Conflicts of Interest:** The authors declare no conflict of interest.

## References

1. Park, H.; Na, K.; Cho, N.; Lee, Y.; Kim, S.-W. A study of the hydrostatic extrusion of copper-clad aluminium tube. *J. Mater. Process. Technol.* **1997**, *67*, 24–28. [[CrossRef](#)]
2. Kim, N.H.; Kang, C.G.; Kwon, H.C. Extrusion process analysis of Al/Cu clad composite materials by finite element method. *J. Korean Soc. Compos. Mater.* **1999**, *43*, 1507–1520.
3. Wu, C.; Hsu, R. Extrusion of three-layer composite hexagonal clad rods. *J. Mater. Process. Technol.* **2002**, *123*, 47–53. [[CrossRef](#)]
4. Kang, C.-G.; Kwon, H. Finite element analysis considering fracture strain of sheath material and die lubricant in extrusion process of Al/Cu clad composites and its experimental investigation. *Int. J. Mech. Sci.* **2002**, *44*, 247–267. [[CrossRef](#)]
5. Lee, J.; Son, H.; Oh, I.; Kang, C.; Yun, C.; Lim, S.; Kwon, H. Fabrication and characterization of Ti-Cu clad materials by indirect extrusion. *J. Mater. Process. Technol.* **2007**, *187–188*, 653–656. [[CrossRef](#)]
6. Sun, X.J.; Tao, J.; Guo, X.Z. Bonding properties of interface in Fe/Al clad tube prepared by explosive welding. *Trans. Nonferrous Met. Soc.* **2011**, *21*, 2175–2180. [[CrossRef](#)]
7. Bae, D.-S.; Kim, S.-M.; We, S.-N.; Bae, D.-H.; Lee, G.-A.; Lee, J.; Kim, Y.-B.; Lee, S. Effect of post heat treatment temperature on interface diffusion layer and bonding force in roll clad Ti/mild steel/Ti material. *Korean J. Met. Mater.* **2012**, *50*, 316–323. [[CrossRef](#)]
8. Lee, S.; Lee, M.-G.; Lee, S.-P.; Lee, G.-A.; Kim, Y.-B.; Lee, J.; Bae, D. Effect of bonding interface on delamination behavior of drawn Cu/Al bar clad material. *Trans. Nonferrous Met. Soc. China* **2012**, *22*, s645–s649. [[CrossRef](#)]
9. Fu, Y.; Jie, J.-C.; Zhang, Y.; Zhong, D.-S.; Li, J.-Z.; Li, T. Microstructure evolution of 3003/4004 clad ingots under diverse physical fields. *Trans. Nonferrous Met. Soc. China* **2013**, *23*, 2496–2501. [[CrossRef](#)]
10. Son, I.-S.; Lee, S.-P.; Lee, J.-K.; Kim, W.-C.; Moon, J.-S.; Lee, S.; Lee, J.; Kim, Y.-B.; Lee, G.-A.; Bae, D.-S. Effect of hydro co-extrusion on microstructure of duo-cast Al 3003/Al 4004 clad materials. *Trans. Nonferrous Met. Soc. China* **2014**, *24*, s75–s80. [[CrossRef](#)]
11. Yan, G.; Mao, F.; Jie, J.; Cao, Z.; Li, T.; Wang, T. Effect of Sr addition on the characteristics of as-cast and rolled 3003/4004 clad aluminum. *J. Alloys Compd.* **2016**, *678*, 201–211. [[CrossRef](#)]
12. Lee, K.S.; Kim, Y.-B.; Lee, S.; Lee, J.-S.; Lee, G.-A.; Lee, S.-P.; Bae, D. Evaluation of intermediate phases formed on the bonding interface of hot pressed Cu/Al clad materials. *Met. Mater. Int.* **2016**, *22*, 849–855. [[CrossRef](#)]
13. Jaradeh, M.M.; Carlberg, T. Solidification studies of 3003 aluminium alloys with Cu and Zr additions. *J. Mater. Sci. Technol.* **2011**, *27*, 615–627. [[CrossRef](#)]

14. Chen, X.; Tian, W.; Li, S.; Yu, M.; Liu, J. Effect of temperature on corrosion behavior of 3003 aluminum alloy in ethylene glycol—Water solution. *Chin. J. Aeronaut.* **2016**, *29*, 1142–1150. [[CrossRef](#)]
15. Flood, S.C.; Hunt, J.D. Modification of Al-Si eutectic alloys with Na. *Met. Sci.* **1981**, *15*, 287–294. [[CrossRef](#)]
16. Shi, W.X.; Gao, B.; Tu, G.F.; Li, S.W. Microstructure and fracture morphology of hypereutectic Al-17.5%Si alloy modified with Nd. *Trans. Nonferrous Met. Soc.* **2011**, *21*, 719–726.
17. Hegde, S.; Prabhu, K.S. Modification of eutectic silicon in Al-Si alloys. *J. Mater. Sci.* **2008**, *43*, 3009–3027. [[CrossRef](#)]
18. Jung, K.; Heo, H.; Park, Y.-C.; Kang, C.-Y.; Lee, J.H. Enhanced corrosion resistance of hypo-eutectic Al-1Mg-xSi alloys against molten sodium attack in high temperature sodium sulfur batteries. *Corros. Sci.* **2015**, *98*, 748–757. [[CrossRef](#)]
19. Fu, Y.; Jie, J.; Wu, L.; Park, J.; Sun, J.; Kim, J.; Li, T. Microstructure and mechanical properties of Al-1Mn and Al-10Si alloy circular clad ingot prepared by direct chill casting. *Mater. Sci. Eng. A* **2013**, *561*, 239–244. [[CrossRef](#)]
20. Liu, N.; Jie, J.; Lu, Y.; Wu, L.; Fu, Y.; Li, T. Characteristics of clad aluminum hollow billet prepared by horizontal continuous casting. *J. Mater. Process. Technol.* **2014**, *214*, 60–66. [[CrossRef](#)]

**Publisher's Note:** MDPI stays neutral with regard to jurisdictional claims in published maps and institutional affiliations.



© 2020 by the authors. Licensee MDPI, Basel, Switzerland. This article is an open access article distributed under the terms and conditions of the Creative Commons Attribution (CC BY) license (<http://creativecommons.org/licenses/by/4.0/>).